Estimating the time course of biomarker changes in Alzheimer's disease

Lars Lau Raket,[1,2] Alexa Pichet Binette,[1] Niklas Mattsson-Carlgren,[1,3,4] Shorena Janelidze,[1] for the Alzheimer's Disease Neuroimaging Initiative, Henrik Zetterberg,[5,6,7,8,9,10] Nicholas J. Ashton,[5,11,12] Kaj Blennow,[5,6] Erik Stomrud,[1,13] Sebastian Palmqvist[1,13] and Oskar Hansson[1,13]

Abstract

Recent advancements in biomarkers have transformed Alzheimer's disease (AD) diagnosis from being purely symptom-based to include biological criteria. With new treatments targeting AD's core biology, understanding the timeline of biological changes is crucial as the disease progresses over decades.

Longitudinal data from amyloid-beta (Aβ) PET and cognitive tests (MMSE and ADAS-cog) from the Alzheimer's Disease Neuroimaging Initiative (n=1,448) and BioFINDER (n=2,088) were used to stage patients against an estimated continuous disease timeline (predicted time since Aβ-PET positivity). The estimated timeline was validated by comparing correlations with unseen biomarkers and cognitive measures against alternative staging approaches. Trajectories for plasma, CSF, MRI, and PET biomarkers, measuring Aβ, tau, and neurodegeneration, were mapped along this AD continuum.

The proposed staging approach was found to produce stronger correlations with unseen cognitive measures and biomarkers compared to alternative staging methods, including amyloid and tau PET clocks (all pairwise $p<0.05$). Findings related to biomarker trajectories were highly consistent across cohorts. The period from Aβ-PET positivity to end-stage AD dementia (MMSE = 0) was estimated at 20-25 years, with a presymptomatic phase of 7-11 years. CSF Aβ42/40 became abnormal about a year before Aβ-PET positivity, CSF p-tau231, p-tau217, and plasma p/np-tau217 1-3 years after, and tau-PET about 8 years after. Neurodegenerative biomarkers, such as hippocampal volume, became clearly abnormal in early dementia stages, 14-16 years after Aβ-PET positivity.

The progression from initial biomarker abnormality to severe AD spans two decades. Disease progression modeling elucidates the evolution of AD biomarkers and cognition, highlighting the relative timing of biomarker abnormalities. These models can determine disease stages, aiding prognosis and evaluation for disease-modifying treatments.

Author affiliations:

1 Clinical Memory Research Unit, Department of Clinical Sciences in Malmö, Lund University, 223 62 Lund, Sweden

2 Eli Lilly and Company, Indianapolis, IN 46285, USA

3 Department of Neurology, Skåne University Hospital, Lund University, 221 85 Lund, Sweden

4 Wallenberg Center for Molecular Medicine, Lund University, 223 62 Lund, Sweden

5 Department of Psychiatry and Neurochemistry, Institute of Neuroscience and Physiology, the Sahlgrenska Academy at the University of Gothenburg, 431 39 Mölndal, Sweden

6 Clinical Neurochemistry Laboratory, Sahlgrenska University Hospital, 431 39 Mölndal, Sweden

7 Department of Neurodegenerative Disease, UCL Institute of Neurology, Queen Square, London WC1N 3BG, UK

8 UK Dementia Research Institute at UCL, London NW1 3BT, UK

9 Hong Kong Center for Neurodegenerative Diseases, Clear Water Bay, Hong Kong 999077, China

10 Wisconsin Alzheimer's Disease Research Center, University of Wisconsin School of Medicine and Public Health, University of Wisconsin-Madison, Madison, WI 53792, USA

11 Banner Alzheimer's Institute and University of Arizona, Phoenix, AZ 85006, USA

12 Banner Sun Health Research Institute, Sun City, AZ 85351, USA

13 Memory Clinic, Skåne University Hospital, 211 46 Malmö, Sweden

Correspondence to: Lars Lau Raket

Clinical Memory Research Unit, Department of Clinical Sciences, Lund University, Sölvegatan 19, 223 62 Lund, Sweden

E-mail: lars.lau_raket@med.lu.se

Running title: Time course of biomarkers changes in AD

Keywords: Alzheimer's disease; biomarkers; disease progression; CSF; PET, amyloid-beta

Introduction

Alzheimer's disease (AD) is biologically defined by the abnormal presence of beta-amyloid (Aβ) plaques and tau-containing neurofibrillary tangles in the brain. AD progresses slowly, starting with a preclinical (presymptomatic) phase where the pathological hallmarks are present with no objectively verified cognition symptoms. This preclinical phase has been suggested to last up to several decades.[1] The preclinical phase is followed by a prodromal phase where cognitive symptoms emerge and increase in severity, followed by dementia where patients lose their ability to independently perform activities of daily living.

Over the last decades, a wide range of biomarkers for AD have become available. These include assays to measure Aβ and tau proteins in cerebrospinal fluid (CSF), positron emission tomography (PET) imaging of AD proteinopathies, volumetric magnetic resonance imaging (MRI), and accurate blood-based biomarkers reproducing CSF findings.[2] Currently available biomarkers enable precise differential diagnosis of AD, and provide staging and prognostic information.[2-6] Based on animal studies, neuropathology and longitudinal biomarker studies, a hypothetical biomarker cascade following the Alzheimer's pathological cascade has been proposed.[7] This model suggests that the prototypical disease trajectory is characterized by initial Aβ plaque accumulation in the brain, followed by spreading of tau pathology and neurodegeneration which in combination leads to cognitive symptoms. This Alzheimer's biomarker cascade has been largely validated and refined in many previous of studies.[8,9]

However, some key unknowns remain. The temporal aspects of AD in relation to biomarker changes has been underappreciated, with most studies either relating biomarkers to other biomarkers[9] or relating them to coarse disease stages based on symptom severity evaluated at single time points.[10] Typical groupings (cognitively unimpaired [CU], mild cognitive impairment [MCI], dementia) represent stages that can last many years with a large severity span within groups, with ambiguous differentiation between groups, and which can be influenced by co-pathologies and premorbid cognitive capacity. Such staging does not reflect the continuous progressive nature of AD, and therefore there are still many unknowns around the fine-scale time evolution of AD.

The current understanding of the evolution of AD in continuous time has relied heavily on studies in autosomal dominant AD. A key reason for this is that knowledge of a subject's mutation type and other characteristics can be used to roughly predict age of symptom onset and progression pattern.[11] This enables calculation of a subject-level disease time scale which in turn enable continuous-time population-level modeling of biomarker trajectories.[12,13] This approach has been instrumental in understanding not only autosomal dominant disease, but also sporadic AD which has many pathophysiological similarities, but also some differences that hamper this extrapolation.[14]

Several methods have been proposed to enable better modeling of biomarker trajectories in sporadic AD. Biologically-consistent estimates of biomarker trajectories along Aβ or tau accumulation as measured by PET have been reported.[9,15,16] To derive a continuous timeline, mimicking the time to symptom onset construct in autosomal dominant AD, amyloid and tau clocks that map PET signals to time and a range of alternative different latent-time disease progression models utilizing both biomarkers and clinical data have been proposed.[17-23] As opposed to the estimated time to symptom onset in autosomal dominant AD, these approaches make use of patterns observed in longitudinal clinical and/or biomarker data to dynamically derive a new latent time scale on which the longitudinal observations are aligned.[24]

In this paper, we propose a disease progression model that utilizes both clinical and Aβ PET data to model the time-course of AD over a latent time scale that represents predicted time since Aβ-PET positivity. We apply the model in well-characterized participants who are either Aβ-negative CU or have biomarker-confirmed AD (all disease stages) in two large cohorts: the

Alzheimer's Disease Neuroimaging Initiative (ADNI) and the Swedish BioFINDER study. Based on the modeling, continuous-time disease stages representing time since Aβ PET positivity were predicted for all subjects, which allowed continuous and time-consistent modeling of biomarker trajectories along the Alzheimer's continuum. We report trajectories for a wide selection of biomarkers measuring aspects of amyloidosis, tauopathy, neurodegeneration and inflammation along predicted time since Aβ positivity, including CSF Aβ42/40 and Aβ PET, tau PET, various p-tau species in CSF and plasma, CSF/plasma neurofilament light (NfL) and volumetric MRI, plasma glial fibrillary acidic protein (GFAP) and CSF sTREM2. These findings shed new light on the fine-scale time evolution of AD.

Materials and methods

Participants

This study included participants from the North American Alzheimer's Disease Neuroimaging Initiative (ADNI) that were recruited under protocols 1, GO, 2 and 3 (NCT00106899, NCT01078636, NCT01231971, and NCT02854033) and participants from the Swedish BioFINDER Study that were recruited under protocols 1 and 2 (NCT01208675 and NCT03174938). All participants in both studies provided written informed consent and the studies were approved by the appropriate ethical review authorities.

ADNI is a multi-site study launched in 2003 as a public-private partnership. The primary goal of ADNI has been to test whether serial MRI, PET, other biological markers, and clinical and neuropsychological assessment can be combined to measure the progression of MCI and early AD. For up-to-date information, see www.adni-info.org.

BioFINDER-1 followed CU, MCI, and dementia participants recruited between 2009 and 2014 for up to 10 years. BioFINDER-2 is an ongoing longitudinal study including participants across the full spectrum of AD, which started in 2017.

The current study used ADNI data collected from 2005 and up to 24 August 2023, all BioFINDER-1 data from 2009 to 12 December 2023 and BioFINDER-2 data collected from 2017 to 24 January 2024.

Inclusion criteria

The inclusion and exclusion criteria for ADNI are described in the study protocols available on the ADNI webpage, and inclusion and exclusion criteria for the BioFINDER studies have been previously described (NCT01208675 and NCT03174938).[25-27] Briefly summarized, in the BioFINDER studies, cognitively unimpaired participants did not fulfill the NIA-AA critiera for MCI or dementia[28] (performed within normal ranges on a large cognitive test battery) and were between 40 and 100 years old. Cognitively impaired participants had been referred to the participating memory clinics at Skåne University Hospital or Ängelholm Hospital in Sweden. Participants with MCI did not fulfil the DSM-5 criteria for major cognitive disorder[29] and performed below normal ranges in at least one cognitive domain as previously described for BioFINDER-1[30] and for BioFINDER-2[27]. All participants understood Swedish to the extent that an interpreter was not necessary.

For the present study, we included participants who at baseline were at least 50 years of age, and had a valid assessment of their cognitive status (ADNI: unimpaired, significant memory concern, early MCI, late MCI, dementia; BioFINDER: unimpaired, subjective cognitive decline [SCD], MCI, dementia), a valid assessment of Aβ status (see details below), and at least one measurement of Aβ PET, MMSE or ADAS-cog.

In BioFINDER, symptomatic participants with an established primary etiology other than AD were excluded. Etiology was assessed based on a thorough longitudinal clinical evaluation, biomarker information, and in some cases genetic information. These clinical evaluation criteria has been described previously.[25] Patients were only excluded based on the clinically established primary etiology, meaning that no effort was done to exclude AD patients with co-pathologies.

CU Aβ-negative (Aβ-) and Aβ-positive (Aβ+) participants were included. Since the goal was to estimate AD-specific trajectories, participants were excluded if they had negative Aβ biomarkers at visits where they showed of objective cognitive impairment (diagnosis of MCI or dementia or CDR global score > 0 or MMSE < 26).

Aβ status

Aβ status (Aβ+/Aβ-) was determined using CSF or PET at every visit where either was available. For CSF, Aβ-positivity was assessed by the Aβ42/40 ratio. In ADNI, Aβ42 and Aβ40 levels were measured on a cobas e 601 analyzer using Roche Elecsys immunoassays (Aβ42/40 positivity cutoff <0.0666) or by 2D-UPLC tandem mass spectrometry[31] (Aβ42/40 positivity cutoff <0.138). In BioFINDER, Aβ42 and Aβ40 were analyzed on a cobas e 601 analyzer using the Roche NeuroToolKit and the cutoff for Aβ-positivity was <0.066 in BioFINDER-1[32] and <0.080 in BioFINDER-2.[33] The PET tracers [^{18}F]florbetapir, [^{18}F]florbetaben and [^{11}C]Pittsburgh Compound B were used to establish Aβ-PET positivity in ADNI using published cut offs by the ADNI PET core, defined by standardized uptake value ratio (SUVR) computed in a composite cortical region referenced to the cerebellum. Cut-offs were 1.11 SUVR for [^{18}F]florbetapir and 1.08 SUVR for [^{18}F]florbetaben and 1.22 for [^{11}C]Pittsburgh Compound B.[34-36] In BioFINDER, Aβ-PET positivity was established using [^{18}F]flutemetamol SUVR in a composite cortical region referenced to the cerebellum with a cutoff of 1.03.[37]

Negative Aβ status was carried backwards, so individuals without a valid Aβ status at baseline but a post-baseline Aβ- status were assumed Aβ- at baseline. Aβ+ status was carried forward.

In some cases, both CSF and PET Aβ biomarkers were available and produced discrepant results (ADNI 229/1954 visits; BioFINDER 271/1078 visits). Discrepant results were primarily in the form of Aβ+ status on CSF and Aβ- status on PET (ADNI 142/229; BioFINDER 217/271) and mostly observed in CU subjects (ADNI 126/229; BioFINDER 196/271), consistent with previous observations that CSF Aβ biomarkers typically become abnormal before PET Aβ biomarkers.[9,38] For CU subjects, we assumed Aβ-positivity if just one of the biomarkers was abnormal. For cognitively impaired subjects, we required Aβ-PET positivity.

Cognitive, functional and clinical outcomes

We used longitudinal Mini-Mental State Examination (MMSE) and Alzheimer's Disease Assessment Scale-cognitive subscale (ADAS-cog)[39] total scores for the disease progression modeling in both cohorts. In ADNI, the 13-item version of ADAS-cog was used, while in BioFINDER, a 2-item version (including immediate and delayed recall) was used.

For exploring the construct validity of the estimated timeline, we used longitudinal scores from the Clinical Dementia Rating – sum of boxes (CDR-SB) and Trail making B in both cohorts. In ADNI, we further used logical memory delayed recall scores.

For validation analyses and for describing the clinical stages associated with the disease progression model analyses, we used clinical diagnosis (CU, MCI, dementia) at each visit. In BioFINDER, clinical diagnosis was not consistently available at all follow-up visits, so we imputed missing diagnoses at visits where we had high certainty of the diagnosis using the following imputation rules: when visits before and after the missing visit had the same diagnosis, all in-between visits with missing diagnosis were interpolated to have the same diagnosis. Cognitively unimpaired status was carried backwards, and diagnoses of dementia were carried forward. When available, CDR global score (0 = CU, 0.5 = MCI, ≥1 = dementia) was used to impute clinical diagnosis at the remaining visits with missing diagnosis.

Plasma, CSF and imaging biomarkers

The following section describes the biomarkers that were used for disease progression modeling, validation or estimation of biomarker trajectories over the AD continuum. The availability of individual biomarkers differed between studies and subject. Sample sizes of available biomarker data will be stated in analyses.

Plasma

In ADNI, included plasma biomarkers were p-tau181, neurofilament light (NfL), and glial fibrillary acidic protein (GFAP), all measured by an electrochemiluminescence immunoassay on the fully automated cobas e 601 (Roche Diagnostics NeuroToolKit),[40] p-tau217, p/np-tau217, defined as the ratio of p-tau217 to np-tau217, and Aβ42/40 measured by liquid chromatography–tandem high-resolution mass spectrometry analysis (PrecivityAD2).[41]

In BioFINDER, included plasma biomarkers were NfL measured using the Roche Diagnostics NeuroToolKit described above, glial fibrillary acidic protein (GFAP) measured using a single molecule array (Simoa)-based assay,[42] p-tau181, p/np-tau181, p-tau217, p/np-tau217 and Aβ42/40 measured by liquid chromatography–tandem high-resolution mass spectrometry analysis,[40,43] and p-tau231 using a Simoa developed at the University of Gothenburg.[44]

CSF

In ADNI, included CSF biomarkers were Aβ42 and Aβ42/40 ratio, p-tau181 and p-tau181/ Aβ42 ratio measured on a cobas e 601 analyzer using Roche Elecsys immunoassays,[45] NfL measured with an enzyme-linked immunosorbent assay (ELISA) from UmanDiagnostic AB,[46] sTREM2 and neurogranin measured with immunoassays using the MSD platform,[47,48] and YKL-40 measured using the MicroVue YKL-40 ELISA.[49]

In BioFINDER, included CSF biomarkers were Aβ42, Aβ42/40 ratio, p-tau181, p-tau181/ Aβ42 ratio, total tau, NfL, neurogranin, and sTREM2 and YKL-40 all measured on a cobas e 601 analyzer using the Roche NeuroToolKit. Furthermore, BioFINDER included CSF p-tau217 measured on the MSD platform using an assay developed by Eli Lilly,[50] and CSF p-tau231 measured on the Simoa platform developed at University of Gothenburg using an antibody from ADx NeuroSciences.[51]

Imaging

In ADNI, included imaging biomarkers were Aβ-PET centiloid computed for the tracers [^{11}C]Pittsburg Compound B, [^{18}F]flortaucipir and [^{18}F]florbetaben based on standardized uptake value (SUVR) ratio in a composite cortical region of interest normalized to the whole cerebellum,[52] tau-PET SUVR using [^{18}F]flortaucipir in Braak regions I, III-IV and V-VI normalized to inferior cerebellar grey matter uptake,[53] [^{18}F]FDG PET SUVR in a meta region of interest,[54] MRI biomarkers of hippocampal and ventricular volume normalized to whole-brain volume[55] and a composite cortical thickness AD-signature[56], all derived using FreeSurfer.

In BioFINDER, included biomarkers were Aβ-PET SUVR using [^{18}F]flutemetamol in a composite cortical region normalized to the cerebellum,[57] tau-PET SUVR using [^{18}F]RO948 in Braak regions I, III-IV and V-VI normalized to the inferior cerebellum grey matter,[57] and MRI biomarkers of hippocampal and ventricular volume normalized to whole-brain volume and composite cortical thickness AD-signature, all derived using FreeSurfer.

Statistical analysis

Disease progression modeling

We developed a semiparametric extension of the multivariate latent-time disease progression model described by Kühnel et al.[58] which estimates trajectories of outcome measures by aligning multivariate subject-level outcome trajectories. As opposed to many other latent-time disease progression models, this modeling approach estimates mean trajectories in a time-consistent manner by using relative visit timings for individual subjects as a scaffold for the time-based estimation. Consequently, a change in values of the mean trajectory associated with a change in time unit (e.g., 1 year) is reflective of the typical change observed over the same time unit for subjects that were matched to that part of the trajectory. The first step of estimating a time-consistent biomarker cascade was to estimate a continuous-time disease trajectory for selected outcomes simultaneously. This involved predicting the continuous-time progression of each subject along this estimated multivariate disease trajectory. The estimated multivariate disease trajectory was based on longitudinal measures of Aβ PET, MMSE and ADAS-cog. The inclusion of both an Aβ biomarker and clinical scales ensures adequate staging information in both pre-symptomatic and symptomatic stages of AD.

The model was defined as follows. Let y_{ijk} denote subject i's observation of the kth outcome measure t_{ij} years after the baseline visit. The mean trajectory θ_k of the kth outcome over the disease continuum was estimated from the model

$$y_{ijk} = \theta_k\left(t_{ij} + s_{\text{bl status}(i)} + s_{\text{bl A}\beta\text{-}(i)} + s_i\right) + x_{ik} + e_{ijk} \quad (1)$$

where we will refer to the time argument $t_{ij} + s_{\text{bl status}(i)} + s_{\text{bl A}\beta\text{-}(i)} + s_i$ that is shared across outcomes as *disease time*.

The model parameters were modeled as follows:

- θ_k was a monotone Hermite spline with 5 degrees of freedom. The spline had 5 + 2 knots. Relative to average baseline disease time of the cognitively normal Aβ+ group, the 5 internal knots were placed at -8.33, 0, 8.33, 16.67, and 25 years with two additional knots replicating the boundary values placed 1 month before and after these respective knots to limit boundary artifacts.

- $s_{\text{bl status}(i)}$ was a fixed effect time-shift describing the average shift in disease time of the baseline status group of subject *i* (i.e., CU, SCD, MCI or dementia in the BioFINDER study)
- $s_{\text{bl A}\beta\text{-}(i)}$ was a fixed effect time-shift describing the average shift in disease time associated with Aβ- status at baseline
- s_i was a random effect time-shift describing the time deviation of subject *i* relative to their baseline group and Aβ+/Aβ- status
- x_{ik} was a random effect intercept describing subject *i*'s consistent deviation in outcome measure *k*, for example the consistent deviation observed for patients with comorbidities or low education that score worse on clinical scales compared to their AD progression stage, an unstructured covariance matrix was used to model the correlation across outcomes
- e_{ijk} was independent identically distributed Gaussian noise with separate variance parameters for each outcome *k*.

To avoid overparameterization, the fixed effect time shifts were anchored such that a disease time of 0 was the time at which a subject on average reached Aβ+ status measured by PET. The predicted disease time thus represents predicted years since Aβ PET positivity. The estimation process is illustrated in Figure 1. All parameters in the model were estimated using maximum likelihood estimation. The maximum a posteriori criterion was used for prediction of random effects. Code for fitting the model is available in the *progmod* R package.[59]

Model validation

The construct validity of the disease progression model was assessed internally in ADNI and BioFINDER based on the predicted disease time's correlation to longitudinal scores from clinical scales measuring cognition and function (Trail making B, Logical memory delayed recall, CDR-SB), and biomarkers related to Aβ, tau and neurodegeneration that were not included in the model. The individual scales and biomarkers were previously described, and biomarkers were grouped into the Aβ, tau and neurodegeneration. The absolute pairwise Spearman correlations to these scales and biomarkers, as well as the domain-weighted average (average of average

absolute pairwise Spearman correlation within each of the four domains: cognition and function, Aβ, tau, neurodegeneration), were compared to alternative longitudinal staging variables related to disease progression. These staging variables included age, clinical diagnosis (0 = CU, 1 = MCI, 2 = dementia), MMSE, ADAS-cog, and Aβ PET. Furthermore, three separate analyses in ADNI compared predicted time since Aβ PET positivity to recently published amyloid and tau clocks estimated based on longitudinal Aβ PET and tau PET data following the algorithm outlined by Milà-Alomà and colleagues,[22] and to the two established continuous-time disease progression models GRACE[18] and LTJMM[60] with model fitted on the same variables as the proposed model based on published implementations. Pairwise comparisons between predicted time since Aβ PET positivity and all other staging measures were done by comparing absolute correlation across all scales and biomarkers with a binomial sign tests. The analysis only included visits where all staging variables were available to ensure comparability (staging variable assigned to same visit, but not required to be collected on the same day, e.g., there were often several weeks difference between clinical scale data collection and PET scans).

Estimating biomarker trajectories

Based on the model (1), each subject had their time since Aβ-PET positivity predicted at all time points. Biomarker trajectories were then analyzed along this predicted disease timeline using a robust quantile mixed-effects spline models with a random Laplace distributed intercept within participants to estimate the median biomarker trajectory.[61] Natural cubic splines with degrees of freedom ranging from 0 (no time dependence), 1 (linear slope) and up to 8 were used to parametrize each median biomarker trajectory, and the model with the lowest Bayesian Information Criterion (BIC) was selected. These biomarkers trajectories were normalized against the median and 95% percentile (in direction of abnormality) of the biomarker values of CU Aβ-negative individuals. The empirical case bootstrap (1000 resamplings) was used to calculate 95% confidence intervals of when individual biomarkers crossed 95% abnormality percentiles.

Results

Study participants

In ADNI, 1963 subjects fulfilled the inclusion criteria and 2277 subjects from BioFINDER fulfilled the inclusion criteria. Among these subjects, 515 subjects in ADNI and 189 subjects in BioFINDER were excluded based on the criteria related to having concurrent Aβ- status and objective cognitive impairment. The baseline characteristics of the 1448 ADNI subjects and 2088 BioFINDER subjects included in the present study are given in Table 1.

Disease progression modeling results and validation

The observed trajectories of the outcome measures plotted against the predicted years since PET Aβ-positivity in the two cohorts are shown in Figure 2. There were substantial overlaps between longitudinal clinical diagnoses stratified by Aβ status along the predicted disease time scale, but the distributions were very similar between cohorts (Figures S1 and S2, Supplementary Material). Sensitivity analyses using only available diagnoses in BioFINDER (data not shown) suggested that the imputation strategy for missing diagnoses in BioFINDER did not affect the estimated distribution of diagnoses along the predicted disease time scale.

Inspection of conditional residuals indicated a symmetric distribution along the predicted disease timeline. However, we observed heterogeneous variance in both cohorts, which increased with disease age (Figure S3 and S4, Supplementary Material). This indicates that there is variability in the datasets not fully accounted for by the model. However, we believe this deviation does not significantly impact the conclusions of our subsequent analyses, as it is more likely to increase uncertainty rather than introduce a meaningful bias. Comparison of the proposed model with sub-models excluding random effects suggested that both the random time shifts and random intercepts captured a very substantial amount of variation in the data. Most notably, excluding the random shift parameter s_i (1 degree of freedom) increased the estimated residual variance in ADNI by 9% for Aβ-PET centiloid, 113% for ADAS-cog (13-item), and 211% for MMSE (Table S1, Supplementary Material). In BioFINDER, the increases in estimated residual variance associated with excluding $s_i$were 10% for Aβ-PET SUVR, 12% for ADAS-cog (2-item), and 94% for MMSE (Table S2, Supplementary Material).

The correlations between the predicted disease time, alternative staging variables and unseen validation variables in ADNI and BioFINDER are given in Tables 2 and 3 respectively. Comparisons of correlations for predicted disease time and an amyloid clock and a tau clock are given in Table S3 in the Supplementary Material and comparisons to other disease progression models are given in Table S4 in the Supplementary Material. To test the validity of the predicted disease time as a single continuous staging measure that effectively captures overall disease progression, the simultaneous pattern of correlations to the full set of validation variables was compared between predicted disease time and the alternative staging variables. In both cohorts, the predicted disease time showed a significantly stronger pattern of correlation to the set of validation variables compared to all other staging variables (all pairwise $p < 0.05$; binomial sign test), including the amyloid PET clock ($p = 0.0034$) and the tau PET clock in ($p = 0.0002$) in ADNI. The predicted disease showed numerically stronger average correlations than GRACE disease time ($p = 0.1796$) and LTJMM disease time ($p = 0.0001$). Notably, predicted disease time and GRACE disease time showed similar correlations for validation variables in the cognition and function and neurodegeneration categories, while predicted disease time showed markedly stronger correlations across all validation variables in the Aβ and tau categories. We note that while predicted disease time had the strongest correlations as a single measure, the validation variables may be affected by multiple independent processes. For example, we found modest but significant partial correlations of age on most validation variables after correcting for predicted disease time, with the smallest partial correlations for AD-specific biomarkers and largest partial correlations across neurodegenerative biomarkers (Table S5, Supplementary Material). We note that correlations were calculated on a common subset of observations where all staging variables were observed to ensure comparability. Figures S5-S8 in the Supplementary Material shows comparisons of predicted disease time, Aβ-PET and tau-PET as staging variables for selected clinical scales and biomarkers.

Biomarker trajectories

For the biomarkers specified in Table 4, longitudinal models for the biomarker trajectories as a function of predicted disease time were fitted. The trajectories were normalized against the median and 95% abnormality quantile for Aβ- CU, to investigate the AD-specific abnormality trajectories. Estimated biomarker abnormality trajectories generally showed consistent patterns

across cohorts (Figure 3; Figure S9, Supplementary Material), and the time at which biomarkers reached abnormality relative to predicted disease time was highly consistent across both cohorts (Figure 4). CSF Aβ42/40 reached 95% abnormality approximately 1 year prior to predicted time of Aβ-PET positivity and was largely consistent with CSF p-tau181/ Aβ42 time of abnormality, but not CSF p-tau181 alone (abnormal 10 years after predicted predicted Aβ PET positivity). CSF p-tau231 and p-tau217, that were only available in BioFINDER, were found to reach 95% abnormality 1 and 3 years after predicted Aβ PET positivity, respectively. Plasma p/np-tau217 reached the 95% abnormality threshold 2-3 years after predicted Aβ PET positivity. In BioFINDER, plasma p-tau217 behaved very similarly to p/np-tau217, while in ADNI, plasma p-tau217 showed approximately 3 years delay in reaching 95% abnormality compared to plasma p/np-tau217. Tau-PET in Braak regions I, II-IV and V-VI reached this abnormality threshold, respectively, 7-9 years, 10-12 years, and 13-15 after Aβ-PET positivity. ADAS-cog and MMSE both became abnormal during the MCI stage of disease (11-15 years after predicted Aβ PET positivity), while volumetric MRI measures of hippocampus and cortical thickness only reached 95% abnormality in the dementia stages of disease (15-16 years after predicted Aβ PET positivity). Sensitivity analyses to assess the impact of different biomarker availability within patients on the estimated abnormality of tau biomarkers found highly consistent patterns of pairwise abnormality timings between biomarkers on subsets of patients with both tau biomarkers available and only limited numerical differences in estimates of abnormality timings based on ADNI data (Section 8, Supplementary Material).

Discussion

In this study, we used latent-time disease progression modeling of Aβ PET and cognitive scale scores to predict years since Aβ PET positivity for subjects in ADNI and BioFINDER. The predicted disease time was shown to outperform other clinical scales, biomarkers and biomarker clocks that are often used for disease staging, including clinical diagnosis, MMSE, amyloid clock and tau clock, in terms of overall strength of correlation to unseen clinical scores and biomarkers representing Aβ, tau, and neurodegeneration. Predicted disease time was also shown to produce numerically stronger correlations to the validation variables than alternative disease staging

models with access to the same information, but the difference did not reach statistical significance compared to the GRACE model. These findings are consistent with the findings of Kühnel and colleagues[58] who found that a similar nonlinear mixed-effects disease progression model produced significantly better predictions of future cognitive trajectories than LTJMM and GRACE.

Compared to conventional staging approaches, predicted disease time has the advantage that a prediction based on any set of observed cross-sectional or longitudinal data will enable calculation of predicted disease time at any future visit, while some staging measures, such as clinical scales or PET-based biomarkers may be difficult to project to visits where they were not assessed. Amyloid and tau PET clocks offer an alternative solution to this problem, but as demonstrated here, these biomarker clocks produce less generalizable stagings than our proposed model. The difference which may be caused by the clocks capturing a single aspect of the disease, that there may be ranges of Aβ and tau PET quantifications that have low predictive value for disease staging (e.g. values below abnormality thresholds, Aβ PET in later symptomatic disease stages), and that the clocks are more affected by noise in the biomarker data due to the more direct translations. Recent work has demonstrated the feasibility of estimating typical biomarker profiles associated with continuous-time disease stage from latent-time disease progression modeling, which in turn enable improved prognostication based on a collection of biomarkers measured at a single visit that reflect different aspects of Alzheimer's disease.[4]

Based on predicted years since Aβ PET positivity, biomarker trajectories were estimated on a joint time scale, and the abnormality of individual biomarkers along the disease timeline were analyzed. This provided new insights, by estimating the temporal relations of when biomarkers and clinical outcome measures typically become abnormal, and the temporal relations between markers of insoluble and soluble pathology. The trajectories of imaging biomarkers were well aligned with the amyloid cascade hypothesis, suggesting that the typical evolution of biomarker profiles along the AD trajectory is one where Aβ biomarkers initially become abnormal, followed by abnormal tau biomarkers and finally abnormal neurodegeneration biomarkers. However, it was found that that amyloidopathy defined using a biofluid-based biomarker (CSF Aβ42/40) was detectable prior to Aβ PET abnormality, which is in agreement with previous results comparing CSF and PET Aβ biomarkers.[38] Further, we found that some biomarkers of

soluble phosphorylated tau became detectably abnormal 1-3 years after Aβ biomarkers (CSF p-tau231, CSP p-tau217, plasma p/np-tau217), many years earlier than tau PET signals became abnormal. P-tau biomarkers (especially p-tau231 but to some extent also p-tau217) have been shown to be very closely associated with early Aβ accumulation,[44,62,63] so the observed signal could reflect early Aβ-induced changes in p-tau and not insoluble tau pathology. Compared to CSF p-tau231 and p-tau217, p-tau181 increased considerably later, reaching 95% abnormality approximately 10 years after Aβ PET. This difference may be partly explained by the effect of different assays analytical protocols for p-tau181 compared to p-tau231 and p-tau217.[9,64] The findings of the present study are largely in agreement with recent findings by Jia and colleagues in a Chinese cohort with 20 years follow-up.[65] In particular, the Chinese study suggested that CSF Aβ-biomarkers became abnormal 14-18 years before diagnosis and CDR-SB scores becoming abnormal 6 years prior to diagnosis, which is consistent with the 12-year gap between abnormality of CSF Aβ42/40 and ADAS-cog in the current study. Differences in timing of abnormality of other CSF markers such as p-tau181 relative to CSF amyloid positivity (3-7 years in Chinese study, 11 years in the present study) may reflect differences in assays, definition of abnormality thresholds, and other methodological differences (including use of imputation of biomarker values in the study by Jia and colleagues).

An important consideration for the estimated time course of biomarker changes presented here is that it does not directly reflect the biological progression of disease but is also influenced by the sensitivity and stability of the biomarker and the natural variation of the biomarker in non-AD populations. The latter feature means that biomarkers that are not specific to AD, such as the neurodegenerative biomarkers considered here, will present as less anomalous compared to biomarkers closer related to AD pathology, but may still track disease progression well within a population of AD patients.

Overall, we showed that despite differences in assays, tracers and processing methods, AD progression was associated with a highly consistent pattern of biomarker progression across two separate cohorts. With the availability of the first approved disease-modifying therapies for Alzheimer's disease in the form of high-clearance Aβ-targeting immunotherapies, biomarkers will play an increasingly important role in verification of the presence of Aβ pathology and early identification of patients. Biomarker-based staging of patients has already been implemented in

some clinical trials through tau-PET-based inclusion criteria,[66,67] in an effort to exclude patients who are early on the disease continuum and thus unlikely to decline during the study period (thus masking a treatment effect) or patients who are late on the disease continuum and thus may be too advanced to fully benefit of the treatment. A natural hypothesis which is being tested in several large studies is that Aβ-targeting immunotherapies would be most efficacious if delivered in the earliest stages of AD, where little tau pathology is present.[68] Resultingly, it is important to know the typical duration of elevated Aβ plaque load without elevated tau. Recently, Therneau and colleagues used an accelerated failure time model with similarities to the approach presented here to estimate the temporal relationship between Aβ-PET and tau-PET.[69] They found the average delay between when Aβ-PET and tau-PET would reach a change point and begin to increase abnormally to be 13.3 years. This duration is slightly longer than the difference between when Aβ-PET and tau-PET became abnormal in the present analysis, with differences of 9 years (Braak I) and 12 years (Braak III-IV) in ADNI and 8 years (Braak I) and 10 years (Braak III-IV) in BioFINDER. The difference in the type of events studied (change in accumulation vs. abnormality relative to Aβ- CU) may have contributed to the differences.

Our work has some limitations. Staging of patients was achieved by modeling under certain assumptions. A key assumption was that AD can be described as evolving around a single multivariate trajectory on a single time scale. However, there may exist AD subtypes with distinct trajectories,[70] and rate of decline and cognitive manifestation can be affected by patient characteristics such as age, comorbidities, and co-pathologies.[4,27,33] In particular, we found that age had substantial partial correlations with neurodegeneration biomarkers after controlling for predicted disease time (Table S5, Supplementary Material). In the present study, such variation was captured by random effects or measurement noise terms. More elaborate modeling of differences in rate of decline and systematic deviations could yield more precise estimates of biomarker evolution. Another assumption of the model was that missing data was not informative, but since patients are more likely to drop out of the study as disease progresses, the disease progression model may rely on a healthier group of subjects and thus estimate a longer disease duration in the later stages of disease than what is typically seen in the real world.[71]

In conclusion, this study used latent-time modeling to analyze longitudinal data from two large cohorts of subjects that were well characterized in terms of their AD status. The continuous-time

staging of patients based on the disease progression model was shown to be superior to existing methods, and by analyzing biomarker trajectories along the resulting AD continuum, we believe our study offers the most accurate estimates of the temporal progression of AD pathology to date.

Data availability

ADNI data is available to qualified academic investigators submitting an online application for access. For more information, please see the ADNI website http://adni.loni.usc.edu/.

Pseudonymized data from BioFINDER will be made available by request from a qualified academic investigator for the sole purpose of replicating procedures and results presented in the article and if data transfer is in agreement with EU legislation on the general data protection regulation and decisions by the Ethical Review Board of Sweden and Region Skåne, which should be regulated in a material transfer agreement.

Acknowledgements

Work at the authors' research center was supported by the National Institute of Aging (R01AG083740), European Research Council (ADG-101096455 and ADG-101053962), Alzheimer's Association (ZEN24-1069572, SG-23-1061717), GHR Foundation, Swedish Research Council (2022-00775, 2023-00356; 2022-01018, and 2019-02397), ERA PerMed (ERAPERMED2021-184), Knut and Alice Wallenberg foundation (2022-0231), Strategic Research Area MultiPark (Multidisciplinary Research in Parkinson's disease) at Lund University, Swedish Alzheimer Foundation (AF-980907), Swedish Brain Foundation (FO2021-0293), Parkinson foundation of Sweden (1412/22), Cure Alzheimer's fund, Rönström Family Foundation, Konung Gustaf V:s och Drottning Victorias Frimurarestiftelse, Skåne University Hospital Foundation (2020-O000028), Regionalt Forskningsstöd (2022-1259) and Swedish federal government under the ALF agreement (2022-Projekt0080 and ALFGBG-71320).

Part of the data collection and sharing of this project was funded by the ADNI (National Institutes of Health Grant U01 AG024904) and DOD ADNI (Department of Defense award

number W81XWH-12-2-0012). ADNI is funded by the National Institute on Aging, the National Institute of Biomedical Imaging and Bioengineering, and through generous contributions from the following: AbbVie, Alzheimer's Association; Alzheimer's Drug Discovery Foundation; Araclon Biotech; BioClinica, Inc.; Biogen; Bristol-Myers Squibb Company; CereSpir, Inc.; Cogstate; Eisai Inc.; Elan Pharmaceuticals, Inc.; Eli Lilly and Company; EuroImmun; F. Hoffmann-La Roche Ltd and its affiliated company Genentech, Inc.; Fujirebio; GE Healthcare; IXICO Ltd.; Janssen Alzheimer Immunotherapy Research & Development, LLC.; Johnson & Johnson Pharmaceutical Research & Development LLC.; Lumosity; Lundbeck; Merck & Co., Inc.; Meso Scale Diagnostics, LLC.; NeuroRx Research; Neurotrack Technologies; Novartis Pharmaceuticals Corporation; Pfizer Inc.; Piramal Imaging; Servier; Takeda Pharmaceutical Company; and Transition Therapeutics. The Canadian Institutes of Health Research is providing funds to support ADNI clinical sites in Canada. Private sector contributions are facilitated by the Foundation for the National Institutes of Health (www.fnih.org). The grantee organization is the Northern California Institute for Research and Education, and the study is coordinated by the Alzheimer's Therapeutic Research Institute at the University of Southern California. ADNI data are disseminated by the Laboratory for Neuro Imaging at the University of Southern California.

Data used in preparation of this article were obtained from the Alzheimer's Disease Neuroimaging Initiative (ADNI) database (adni.loni.usc.edu). As such, the investigators within the ADNI contributed to the design and implementation of ADNI and/or provided data but did not participate in analysis or writing of this report. A complete listing of ADNI investigators can be found at: http://adni.loni.usc.edu/wp-content/uploads/how_to_apply/ADNI_Acknowledgement_List.pdf

Competing interests

LLR is a full-time employee and shareholder of Eli Lilly and Company. SP has acquired research support (for the institution) from ki elements / ADDF. In the past 2 years, he has received consultancy/speaker fees from Bioartic, Biogen, Eisai, Lilly, and Roche. APB, NMC, and ES has no disclosures. HZ has served at scientific advisory boards and/or as a consultant for Abbvie, Acumen, Alector, Alzinova, ALZPath, Amylyx, Annexon, Apellis, Artery Therapeutics,

AZTherapies, Cognito Therapeutics, CogRx, Denali, Eisai, LabCorp, Merry Life, Nervgen, Novo Nordisk, Optoceutics, Passage Bio, Pinteon Therapeutics, Prothena, Red Abbey Labs, reMYND, Roche, Samumed, Siemens Healthineers, Triplet Therapeutics, and Wave, has given lectures in symposia sponsored by Alzecure, Biogen, Cellectricon, Fujirebio, Lilly, Novo Nordisk, and Roche, and is a co-founder of Brain Biomarker Solutions in Gothenburg AB (BBS), which is a part of the GU Ventures Incubator Program (outside submitted work). NJA has given lectures in symposia sponsored by Quanterix, Eli Lilly, and Biogen. KB has served as a consultant and on advisory boards for Acumen, ALZPath, BioArctic, Biogen, Eisai, Lilly, Moleac Pte. Ltd, Novartis, Ono Pharma, Prothena, Roche Diagnostics, and Siemens Healthineers; serving on data monitoring committees for Julius Clinical and Novartis; giving lectures, producing educational materials, and participating in educational programs for AC Immune, Biogen, Celdara Medical, Eisai, and Roche Diagnostics; and being a co-founder of Brain Biomarker Solutions in Gothenburg AB (BBS), which is a part of the GU Ventures Incubator Program, outside the submitted work. OH has acquired research support (for the institution) from ADx, AVID Radiopharmaceuticals, Biogen, Eli Lilly, Eisai, Fujirebio, GE Healthcare, Pfizer, and Roche and consultancy/speaker fees from AC Immune, Amylyx, Alzpath, BioArctic, Biogen, Cerveau, Eisai, Eli Lilly, Fujirebio, Merck, Novartis, Novo Nordisk, Roche, Sanofi, and Siemens outside the submitted work.

Supplementary material

Supplementary material is available at *Brain* online.

References

1. Dubois B, Hampel H, Feldman HH, et al. Preclinical Alzheimer's disease: definition, natural history, and diagnostic criteria. *Alzheimer's & Dementia*. 2016;12(3):292-323.

2. Hansson O. Biomarkers for neurodegenerative diseases. *Nat Med*. Jun 2021;27(6):954-963. doi:10.1038/s41591-021-01382-x

3. Simrén J, Leuzy A, Karikari TK, et al. The diagnostic and prognostic capabilities of plasma biomarkers in Alzheimer's disease. *Alzheimer's & Dementia*. 2021;17(7):1145-1156.

4. Kühnel L, Bouteloup V, Lespinasse J, et al. Personalized prediction of progression in pre-dementia patients based on individual biomarker profile: A development and validation study. *Alzheimer's & Dementia*. 2021;17(12):1938-1949.

5. Zetterberg H, Bendlin BB. Biomarkers for Alzheimer's disease—preparing for a new era of disease-modifying therapies. *Molecular psychiatry*. 2021;26(1):296-308.

6. Hansson O. Biomarkers for neurodegenerative diseases. *Nat Med*. 2021;27(6):954-963.

7. Jack Jr CR, Knopman DS, Jagust WJ, et al. Hypothetical model of dynamic biomarkers of the Alzheimer's pathological cascade. *The Lancet Neurology*. 2010;9(1):119-128.

8. Jack Jr CR, Knopman DS, Jagust WJ, et al. Tracking pathophysiological processes in Alzheimer's disease: an updated hypothetical model of dynamic biomarkers. *The lancet neurology*. 2013;12(2):207-216.

9. Palmqvist S, Insel PS, Stomrud E, et al. Cerebrospinal fluid and plasma biomarker trajectories with increasing amyloid deposition in Alzheimer's disease. *EMBO molecular medicine*. 2019;11(12):e11170.

10. Jansen WJ, Janssen O, Tijms BM, et al. Prevalence Estimates of Amyloid Abnormality Across the Alzheimer Disease Clinical Spectrum. *JAMA Neurol*. Mar 1 2022;79(3):228-243. doi:10.1001/jamaneurol.2021.5216

11. Ryman DC, Acosta-Baena N, Aisen PS, et al. Symptom onset in autosomal dominant Alzheimer disease: a systematic review and meta-analysis. *Neurology*. Jul 15 2014;83(3):253-60. doi:10.1212/WNL.0000000000000596

12. Schindler SE, Fagan AM. Autosomal dominant Alzheimer disease: a unique resource to study CSF biomarker changes in preclinical AD. *Frontiers in neurology*. 2015;6:142.

13. Fagan AM, Xiong C, Jasielec MS, et al. Longitudinal change in CSF biomarkers in autosomal-dominant Alzheimer's disease. *Science translational medicine*. 2014;6(226):226ra30-226ra30.

14. Morris JC, Weiner M, Xiong C, et al. Autosomal dominant and sporadic late onset Alzheimer disease share a common in vivo pathophysiology. *Brain*. 2022;

15. Therriault J, Pascoal TA, Lussier FZ, et al. Biomarker modeling of Alzheimer's disease using PET-based Braak staging. *Nature Aging*. 2022:1-10.

16. Milà-Alomà M, Ashton NJ, Shekari M, et al. Plasma p-tau231 and p-tau217 as state markers of amyloid-β pathology in preclinical Alzheimer's disease. *Nat Med*. 2022;28(9):1797-1801.

17. Jedynak BM, Liu B, Lang A, Gel Y, Prince JL, Neuroimaging AD. A computational method for computing an Alzheimer's disease progression score; experiments and validation with the ADNI data set. *Neurobiol Aging*. Jan 2015;36:S178-S184. doi:10.1016/j.neurobiolaging.2014.03.043

18. Donohue MC, Jacqmin-Gadda H, Le Goff M, et al. Estimating long-term multivariate progression from short-term data. *Alzheimers Dement*. Oct 2014;10(5):S400-S410. doi:10.1016/j.jalz.2013.10.003

19. Raket LL. Statistical Disease Progression Modeling in Alzheimer Disease. *Front Big Data*. Aug 12 2020;3doi:ARTN 24

10.3389/fdata.2020.00024

20. Schindler SE, Li Y, Buckles VD, et al. Predicting symptom onset in sporadic Alzheimer disease with amyloid PET. *Neurology*. 2021;97(18):e1823-e1834.

21. Insel PS, Donohue MC, Berron D, Hansson O, Mattsson-Carlgren N. Time between milestone events in the Alzheimer's disease amyloid cascade. *Neuroimage*. Feb 15 2021;227:117676. doi:10.1016/j.neuroimage.2020.117676

22. Milà-Alomà M, Tosun D, Schindler SE, et al. Timing of changes in Alzheimer's disease plasma biomarkers as assessed by amyloid and tau PET clocks. *Annals of Neurology*. 2025;

23. Betthauser TJ, Bilgel M, Koscik RL, et al. Multi-method investigation of factors influencing amyloid onset and impairment in three cohorts. *Brain*. 2022;145(11):4065-4079.

24. Young AL, Oxtoby NP, Garbarino S, Fox NC, Barkhof F, Schott JM, Alexander DC. Data-driven modelling of neurodegenerative disease progression: thinking outside the black box. *Nature Reviews Neuroscience*. 2024:1-20.

25. Palmqvist S, Janelidze S, Quiroz YT, et al. Discriminative accuracy of plasma phospho-tau217 for Alzheimer disease vs other neurodegenerative disorders. *Jama*. 2020;324(8):772-781.

26. Palmqvist S, Tideman P, Cullen N, et al. Prediction of future Alzheimer's disease dementia using plasma phospho-tau combined with other accessible measures. *Nat Med*. Jun 2021;27(6):1034-1042. doi:10.1038/s41591-021-01348-z

27. Palmqvist S, Rossi M, Hall S, et al. Cognitive effects of Lewy body pathology in clinically unimpaired individuals. *Nat Med*. Aug 2023;29(8):1971-1978. doi:10.1038/s41591-023-02450-0

28. Jack CR, Jr., Bennett DA, Blennow K, et al. NIA-AA Research Framework: Toward a biological definition of Alzheimer's disease. *Alzheimers Dement*. Apr 2018;14(4):535-562. doi:10.1016/j.jalz.2018.02.018

29. American Psychiatric Association D, Association AP. *Diagnostic and statistical manual of mental disorders: DSM-5*. vol 5. American psychiatric association Washington, DC; 2013.

30. Petrazzuoli F, Vestberg S, Midlov P, Thulesius H, Stomrud E, Palmqvist S. Brief Cognitive Tests Used in Primary Care Cannot Accurately Differentiate Mild Cognitive Impairment from Subjective Cognitive Decline. *J Alzheimers Dis*. 2020;75(4):1191-1201. doi:10.3233/JAD-191191

31. Korecka M, Waligorska T, Figurski M, et al. Qualification of a surrogate matrix-based absolute quantification method for amyloid-β 42 in human cerebrospinal fluid using 2D UPLC-tandem mass spectrometry. *Journal of Alzheimer's Disease*. 2014;41(2):441-451.

32. Palmqvist S, Stomrud E, Cullen N, et al. An accurate fully automated panel of plasma biomarkers for Alzheimer's disease. *Alzheimers Dement*. Aug 11 2022;doi:10.1002/alz.12751

33. Quadalti C, Palmqvist S, Hall S, et al. Clinical effects of Lewy body pathology in cognitively impaired individuals. *Nat Med*. Aug 2023;29(8):1964-1970. doi:10.1038/s41591-023-02449-7

34. Jagust WJ, Bandy D, Chen K, et al. The Alzheimer's Disease Neuroimaging Initiative positron emission tomography core. *Alzheimers Dement*. May 2010;6(3):221-9. doi:10.1016/j.jalz.2010.03.003

35. Landau S, Murphy A, Ward T, Jagust W. Florbetapir processing methods. *Alzheimer's Disease Neuroimaging Initiative*. 2021;

36. Landau S, Murphy A, Ward T, Jagust W. Florbetaben processing methods. *Alzheimer's Disease Neuroimaging Initiative*. 2021;

37. Ossenkoppele R, Pichet Binette A, Groot C, et al. Amyloid and tau PET-positive cognitively unimpaired individuals are at high risk for future cognitive decline. *Nat Med*. Nov 2022;28(11):2381-2387. doi:10.1038/s41591-022-02049-x

38. Palmqvist S, Mattsson N, Hansson O, Alzheimer's Disease Neuroimaging I. Cerebrospinal fluid analysis detects cerebral amyloid-beta accumulation earlier than positron emission tomography. *Brain*. Apr 2016;139(Pt 4):1226-36. doi:10.1093/brain/aww015

39. Rosen WG, Mohs RC, Davis KL. A new rating scale for Alzheimer's disease. *Am J Psychiatry*. Nov 1984;141(11):1356-64. doi:10.1176/ajp.141.11.1356

40. Johnson SC, Suárez-Calvet M, Suridjan I, et al. Identifying clinically useful biomarkers in neurodegenerative disease through a collaborative approach: the NeuroToolKit. *Alzheimer's Research & Therapy*. 2023;15(1):25.

41. Meyer MR, Kirmess KM, Eastwood S, et al. Clinical validation of the PrecivityAD2 blood test: A mass spectrometry-based test with algorithm combining% p-tau217 and Aβ42/40 ratio to identify presence of brain amyloid. *Alzheimer's & Dementia*. 2024;20(5):3179-3192.

42. Pereira JB, Janelidze S, Smith R, et al. Plasma GFAP is an early marker of amyloid-beta but not tau pathology in Alzheimer's disease. *Brain*. Dec 16 2021;144(11):3505-3516. doi:10.1093/brain/awab223

43. Barthélemy NR, Salvadó G, Schindler SE, et al. Highly accurate blood test for Alzheimer's disease is similar or superior to clinical cerebrospinal fluid tests. *Nature medicine*. 2024;30(4):1085-1095.

44. Ashton NJ, Janelidze S, Mattsson-Carlgren N, et al. Differential roles of Abeta42/40, p-tau231 and p-tau217 for Alzheimer's trial selection and disease monitoring. *Nature medicine*. Dec 2022;28(12):2555-2562. doi:10.1038/s41591-022-02074-w

45. Lifke V, Kollmorgen G, Manuilova E, et al. Elecsys® Total-Tau and Phospho-Tau (181P) CSF assays: analytical performance of the novel, fully automated immunoassays for quantification of tau proteins in human cerebrospinal fluid. *Clinical biochemistry*. 2019;72:30-38.

46. Nordlund A, Rolstad S, Hellström P, Sjögren M, Hansen S, Wallin A. The Goteborg MCI study: mild cognitive impairment is a heterogeneous condition. *Journal of Neurology, Neurosurgery & Psychiatry*. 2005;76(11):1485-1490.

47. Kleinberger G, Yamanishi Y, Suárez-Calvet M, et al. TREM2 mutations implicated in neurodegeneration impair cell surface transport and phagocytosis. *Science translational medicine*. 2014;6(243):243ra86-243ra86.

48. Portelius E, Zetterberg H, Skillbäck T, et al. Cerebrospinal fluid neurogranin: relation to cognition and neurodegeneration in Alzheimer's disease. *Brain*. 2015;138(11):3373-3385.

49. Sutphen C, Macy E, Ladenson J, Fagan A. Longitudinal analysis of cerebrospinal fluid Visinin-like protein-1, chitinase-3 like-1, synaptosomal-associated protein 25 and neurogranin. Alzheimer's Disease Neuroimaging Initiative. 2011.

50. Janelidze S, Stomrud E, Smith R, et al. Cerebrospinal fluid p-tau217 performs better than p-tau181 as a biomarker of Alzheimer's disease. *Nat Commun*. Apr 3 2020;11(1):1683. doi:10.1038/s41467-020-15436-0

51. Leuzy A, Janelidze S, Mattsson-Carlgren N, et al. Comparing the clinical utility and diagnostic performance of CSF P-Tau181, P-Tau217, and P-Tau231 assays. *Neurology*. 2021;97(17):e1681-e1694.

52. Bourgeat P, Doré V, Burnham SC, et al. β-amyloid PET harmonisation across longitudinal studies: Application to AIBL, ADNI and OASIS3. *NeuroImage*. 2022;262:119527.

53. Landau S, Jagust W. Flortaucipir (AV-1451) processing methods. *Alzheimer's Disease Neuroimaging Initiative*. 2016;

54. Landau SM, Harvey D, Madison CM, et al. Associations between cognitive, functional, and FDG-PET measures of decline in AD and MCI. *Neurobiology of aging*. 2011;32(7):1207-1218.

55. Jack Jr CR, Bernstein MA, Fox NC, et al. The Alzheimer's disease neuroimaging initiative (ADNI): MRI methods. *Journal of Magnetic Resonance Imaging: An Official Journal of the International Society for Magnetic Resonance in Medicine*. 2008;27(4):685-691.

56. Jack Jr CR, Wiste HJ, Weigand SD, et al. Defining imaging biomarker cut points for brain aging and Alzheimer's disease. *Alzheimer's & Dementia*. 2017;13(3):205-216.

57. Pichet Binette A, Franzmeier N, Spotorno N, et al. Amyloid-associated increases in soluble tau relate to tau aggregation rates and cognitive decline in early Alzheimer's disease. *Nat Commun*. Nov 4 2022;13(1):6635. doi:10.1038/s41467-022-34129-4

58. Kuhnel L, Berger AK, Markussen B, Raket LL. Simultaneous modeling of Alzheimer's disease progression via multiple cognitive scales. *Statistics in Medicine*. Jun 30 2021;40(14):3251-3266. doi:10.1002/sim.8932

59. *progmod – Disease progression modeling based on nonlinear mixed effects modeling*. 2023. https://github.com/larslau/progmod

60. Li D, Iddi S, Thompson WK, Donohue MC, Alzheimer's Disease Neuroimaging I. Bayesian latent time joint mixed effect models for multicohort longitudinal data. *Stat Methods Med Res*. Mar 2019;28(3):835-845. doi:10.1177/0962280217737566

61. Geraci M. Linear quantile mixed models: the lqmm package for Laplace quantile regression. *Journal of Statistical Software*. 2014;57:1-29.

62. Mattsson N, Andersson E, Janelidze S, et al. Aβ deposition is associated with increases in soluble and phosphorylated tau that precede a positive Tau PET in Alzheimer's disease. *Science Advances*. 15 Apr 2020;6(16):eaaz2387.

63. Mattsson-Carlgren N, Janelidze S, Bateman RJ, et al. Soluble P-tau217 reflects amyloid and tau pathology and mediates the association of amyloid with tau. *EMBO Mol Med*. Jun 7 2021;13(6):e14022. doi:10.15252/emmm.202114022

64. Palmqvist S, Zetterberg H, Mattsson N, et al. Detailed comparison of amyloid PET and CSF biomarkers for identifying early Alzheimer disease. *Neurology*. Oct 6 2015;85(14):1240-9. doi:10.1212/WNL.0000000000001991

65. Jia J, Ning Y, Chen M, et al. Biomarker Changes during 20 Years Preceding Alzheimer's Disease. *N Engl J Med*. Feb 22 2024;390(8):712-722. doi:10.1056/NEJMoa2310168

66. Mintun MA, Wessels AM, Sims JR. Donanemab in Early Alzheimer's Disease. Reply. *N Engl J Med*. Aug 12 2021;385(7):667. doi:10.1056/NEJMc2109455

67. Sims JR, Zimmer JA, Evans CD, et al. Donanemab in early symptomatic Alzheimer disease: the TRAILBLAZER-ALZ 2 randomized clinical trial. *JAMA*. 2023;

68. Rafii MS, Sperling RA, Donohue MC, et al. The AHEAD 3-45 Study: Design of a prevention trial for Alzheimer's disease. *Alzheimer's & Dementia*. 2023;19(4):1227-1233.

69. Therneau TM, Knopman DS, Lowe VJ, et al. Relationships between β-amyloid and tau in an elderly population: An accelerated failure time model. *Neuroimage*. 2021;242:118440.

70. Vogel JW, Young AL, Oxtoby NP, et al. Four distinct trajectories of tau deposition identified in Alzheimer's disease. *Nature medicine*. 2021;27(5):871-881.

71. Rouanet A, Avila-Rieger J, Dugravot A, et al. How selection over time contributes to the inconsistency of the association between sex/gender and cognitive decline across cognitive aging cohorts. *American journal of epidemiology*. 2022;191(3):441-452.

Figure legends

Figure 1 Illustration of the alignment of observed samples from four subjects against estimated trajectories of outcomes (dotted lines) along the predicted disease time scale. Line colors differentiate individual subjects while point colors show the diagnosis of a subject at a given visit. The dotted mean trajectories are estimated simultaneously with the alignment of individual subject trajectories based on all available data.

Figure 2 Participants' longitudinal trajectories of the three measures used to build the disease progression model. Aβ PET, ADAS-cog and MMSE in ADNI (N = 1448) and BioFINDER (N = 2088) plotted against predicted time since Aβ-PET positivity. The time scale is measured in years with 0 is anchored at the time of average Aβ positivity as assessed by PET.

Figure 3 Biomarker trajectories showing abnormality relative to cognitively unimpaired Aβ-negative subjects. Figure shows measures included in the disease progression model, plasma biomarkers, CSF biomarkers, MRI biomarkers, and PET biomarkers.

Figure 4 Estimated time point of when different measures on average reach 95% abnormality threshold relative to cognitively unimpaired Aβ-negative subjects. A. ADNI and B. BioFINDER. Lines represent 95% confidence intervals computed using the empirical case bootstrap.

Table 1 Baseline characteristics of subjects in ADNI and BioFINDER

	ADNI	BioFINDER
N	1448	2088
Female (%)	728 (50%)	1199 (57%)
Education (years)	16 [14, 18]	12 [10, 15]
Age (years)	72.9 [68.1, 77.9]	72.4 [66.6, 76.9]
Follow-up time (years)	2.8 [1.0, 4.3]	3.8 [1.6, 6.2]
Cognitively unimpaired at baseline		
N	677	1436
Female (%)	395 (58%)	855 (60%)
APOE ε4 carriers (%)	200 (32%)	530 (37%)
Education (years)	16 [15, 18]	12 [10, 15]
Age (years)	71.4 [67.1, 76.3]	71.4 [65.0, 76.4]
Aβ-positive (%)	293 (43%)	499 (35%)
MMSE	29 [29, 30]	29 [28, 30]
MCI at baseline		
N	501	400
Female (%)	212 (42%)	202 (50%)
APOE ε4 carriers (%)	314 (66%)	286 (72%)
Education (years)	16 [14, 18]	12 [9, 15]
Age (years)	73.9 [68.8, 78.2]	73.8 [69.3, 77.2]
Aβ-positive (%)	478 (100%)	400 (100%)
MMSE	28 [26, 29]	27 [25, 28]
Dementia at baseline		
N	270	252
Female (%)	121 (45%)	142 (56%)
APOE ε4 carriers (%)	194 (75%)	179 (71%)
Education (years)	16 [13, 18]	12 [9, 14]
Age (years)	74.4 [69.1, 79.6]	75.1 [70.7, 78.5]
Aβ-positive (%)	265 (100%)	252 (100%)
MMSE	23 [21, 25]	21 [18, 24]

Continuous measures are given as median [interquartile range]. MMSE = Mini Mental State Examination.

Table 2 Spearman correlations (absolute value) between staging variables and unseen validation variables in ADNI

Domain	Validation variable	Staging variables					
		Age	Diagnosis[a]	MMSE	ADAS-cog	Aβ PET	Predicted disease time
Cognition and function	Trail making B (*n* = 2119)	0.29	0.53	0.53	**0.58**	0.45	0.57
	Logical memory delayed recall (*n* = 2175)	0.06	**0.77**	0.66	0.75	0.55	0.70
	CDR-SB (n = 2178)	0.11	**0.93**	0.68	0.74	0.65	0.82
Aβ	Plasma Aβ42/40 (*n* = 615)	0.04	0.25	0.15	0.15	**0.42**	0.39
	CSF Aβ42/40 (*n* = 542)	0.23	0.55	0.38	0.43	0.78	**0.81**
Tau	Plasma p-tau181 (*n* = 615)	0.28	0.42	0.35	0.40	0.60	**0.66**
	Plasma p/np-tau217 (n = 618)	0.14	0.56	0.45	0.50	0.78	**0.81**
	CSF p-tau181 (*n* = 1340)	0.15	0.48	0.39	0.44	0.58	**0.60**
	Tau PET Braak III-IV SUVR (*n* = 661)	0.08	0.56	0.38	0.54	0.60	**0.64**
Neurodegeneration	Plasma NfL (*n* = 615)	**0.51**	0.24	0.22	0.30	0.27	0.41
	MRI hippocampus volume (*n* = 1802)	0.38	0.57	0.51	0.58	0.43	**0.59**
	MRI ventricle volume (*n* = 1761)	**0.45**	0.29	0.29	0.35	0.26	0.38
	MRI AD thickness signature (*n* = 875)	0.34	0.55	0.55	0.62	0.43	**0.65**
	FDG PET SUVR (*n* = 1045)	0.13	0.57	0.55	0.65	0.44	**0.67**
Domain-weighted average		0.20	0.53	0.43	0.49	0.54	**0.63**

Correlations are computed on the subset of data with complete data for all staging variables. *n* denotes number of observations of the validation variable. Bold text indicates the strongest correlation across staging variables. MMSE = Mini Mental State Examination; ADAS-cog = Alzheimer's Disease Assessment Scale – cognitive subscale; CDR-SB = Clinical Dementia Rating – Sum of Boxes; SUVR = Standardized Uptake Value Ratio; AD = Alzheimer's disease, MCI = Mild Cognitive Impairment.

[a]Diagnosis coded numerically as 0 = cognitively unimpaired, 1 = MCI, 2 = dementia.

Table 3 Spearman correlations (absolute value) between staging variables and unseen validation variables in BioFINDER

Domain	Validation variable	Staging variables					
		Age	Diagnosis[a]	MMSE	ADAS-cog	Aβ PET	Predicted disease time
Cognition and function	Trail making B (*n* = 1431)	0.45	0.49	0.45	**0.52**	0.45	0.49
	CDR-SB (n = 328)	0.02	**0.89**	0.63	0.75	0.67	0.79
Aβ	Plasma Aβ42/40 (*n* = 487)	0.16	0.33	0.18	0.35	0.49	**0.52**
	CSF Aβ42/40 (*n* = 1091)	0.25	0.53	0.33	0.46	0.78	**0.81**
Tau	Plasma p-tau181 (n = 763)	0.45	0.34	0.28	0.38	**0.50**	0.46
	Plasma p/np-tau 217 (n = 761)	0.32	0.57	0.35	0.49	**0.78**	0.76
	CSF p-tau181 (*n* = 1095)	0.31	0.45	0.32	0.45	0.60	**0.61**
	CSF p-tau 217 (*n* = 269)	0.06	0.63	0.51	0.63	0.81	**0.81**
	CSF p-tau 231 (*n* = 440)	0.39	0.54	0.37	0.51	0.71	**0.75**
	Tau PET Braak III-IV SUVR (*n* = 1250)	0.31	0.51	0.37	0.46	0.58	**0.58**
Neurodegeneration	Plasma NfL (*n* = 236)	0.27	0.24	0.17	0.19	0.20	**0.28**
	CSF NfL (*n* = 728)	0.51	0.43	0.36	0.46	0.49	**0.51**
	CSF neurogranin (*n* = 726)	0.18	0.26	0.24	0.30	0.35	**0.38**
	MRI hippocampus volume (*n* = 1226)	0.53	0.48	0.39	**0.55**	0.47	0.50
	MRI ventricle volume (*n* = 1226)	**0.57**	0.33	0.28	0.40	0.33	0.35
	MRI AD thickness signature (*n* = 1226)	0.46	0.48	0.36	0.48	0.47	**0.52**
Domain-weighted average		0.29	0.50	0.37	0.48	0.56	**0.60**

Correlations are computed on the subset of data with complete data for all staging variables. *n* denotes number of observations of the validation variable. Bold text indicates the strongest correlation across staging variables. MMSE = Mini Mental State Examination; ADAS-cog = Alzheimer's Disease Assessment Scale – cognitive subscale; CDR-SB = Clinical Dementia Rating – Sum of Boxes; SUVR = Standardized Uptake Value Ratio; AD = Alzheimer's disease, MCI = Mild Cognitive Impairment.

[a]Diagnosis coded numerically as 0 = cognitively unimpaired, 1 = MCI, 2 = dementia.

Table 4 Available longitudinal biomarker data and correlation to predicted disease time in the ADNI and BioFINDER cohorts

	ADNI			BioFINDER		
	Measurements	**Subjects**	**Spearman ρ with predicted disease time**	**Measurements**	**Subjects**	**Spearman ρ with predicted disease time**
Model measures						
Aβ PET	2288	1138	0.82	2040	1339	0.83
ADAS-cog	6237	1447	0.82	6472	2071	0.73
MMSE	6322	1448	-0.76	6840	2088	-0.72
Plasma						
Aβ42/40	687	233	-0.38	638	638	-0.51
P-tau181	686	233	0.66	1006	1006	0.59
P/Np-tau181	—	—	—	1006	1006	0.66
P-tau217	690	233	0.80	1004	1004	0.83
P/Np-tau217	690	233	0.81	1004	1004	0.84
P-tau231	—	—	—	922	922	0.66
NfL	686	223	0.42	1303	505	0.27
GFAP	684	233	0.54	943	943	0.53
CSF						
Aβ42	2283	1213	-0.69	2702	1888	-0.71
Aβ42/40	684	416	-0.80	2702	1888	-0.78
P-tau181/Aβ42	2283	1213	0.78	2707	1893	0.63
P-tau181	2283	1213	0.57	2707	1893	0.63
P-tau217	—	—	—	1594	799	0.74
P-tau231	—	—	—	610	610	0.80
Total tau	2284	1213	0.53	2707	1893	0.58
NfL	325	325	0.42	2252	1438	0.54
Neurogranin	325	325	0.33	2252	1436	0.54
YKL-40	463	121	0.12	2254	1440	0.29
sTREM2	1275	745	-0.01	2255	1441	0.15
MRI						
Ventricles volume	5343	1411	0.39	2080	1258	0.44
Hippocampus volume	5106	1393	-0.63	2080	1258	-0.62
AD thickness signature	3781	839	-0.68	2080	1258	-0.66
PET						
Aβ PET SUVR	2288	1138	0.82	2040	1339	0.83
Tau PET SUVR (Braak I)	891	533	0.71	2089	1254	0.75
Tau PET SUVR (Braak III-IV)	891	533	0.66	2089	1254	0.72
Tau PET SUVR (Braak V-VI)	891	533	0.52	2089	1254	0.55
FDG PET SUVR	1987	976	-0.68	—	—	—

ADAS-cog = Alzheimer's Disease Assessment Scale – cognitive subscale; MMSE = Mini Mental State Examination; AD = Alzheimer's disease; SUVR = Standardized Uptake Value Ratio.

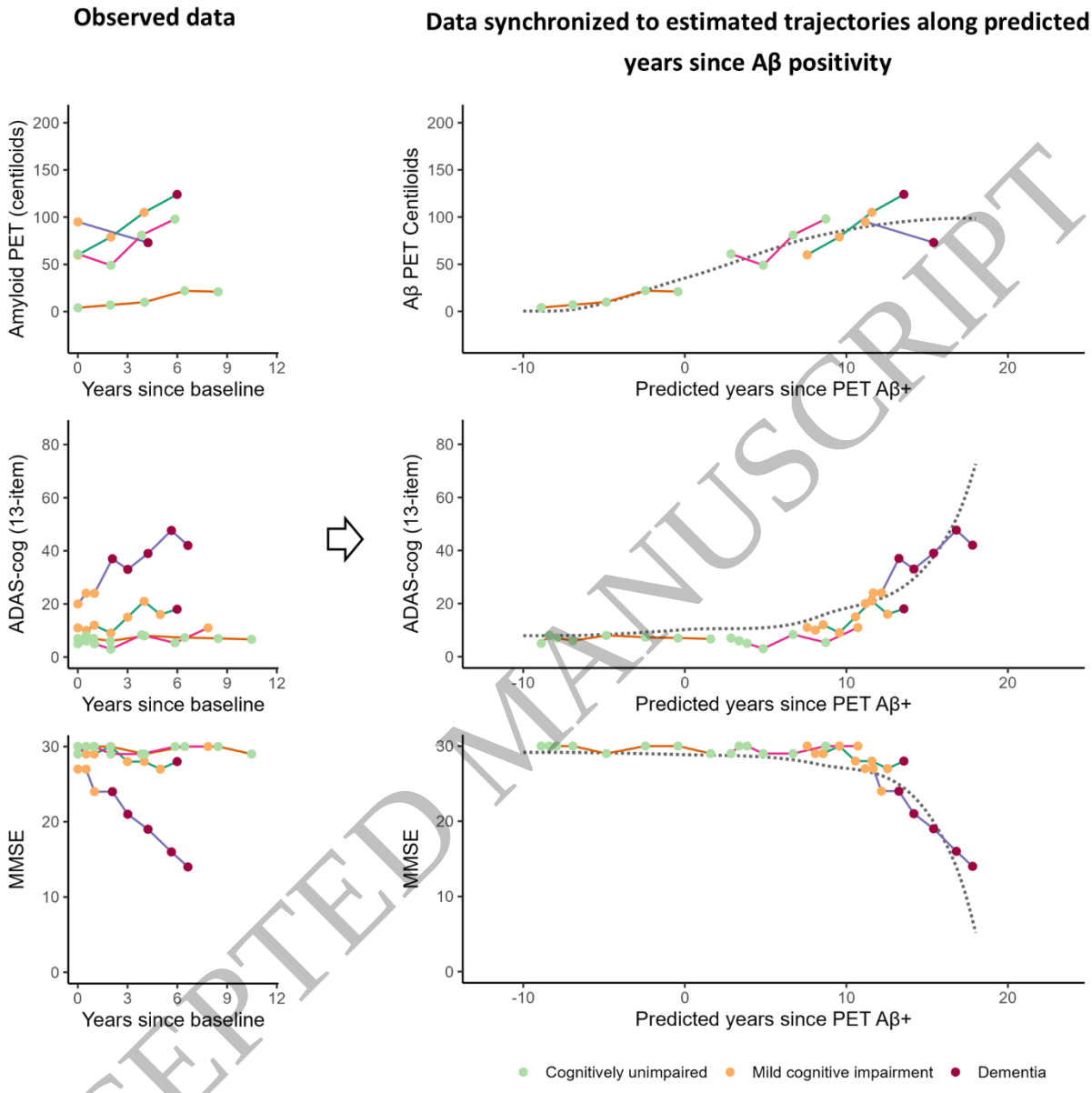

Figure 1
163x161 mm (x DPI)

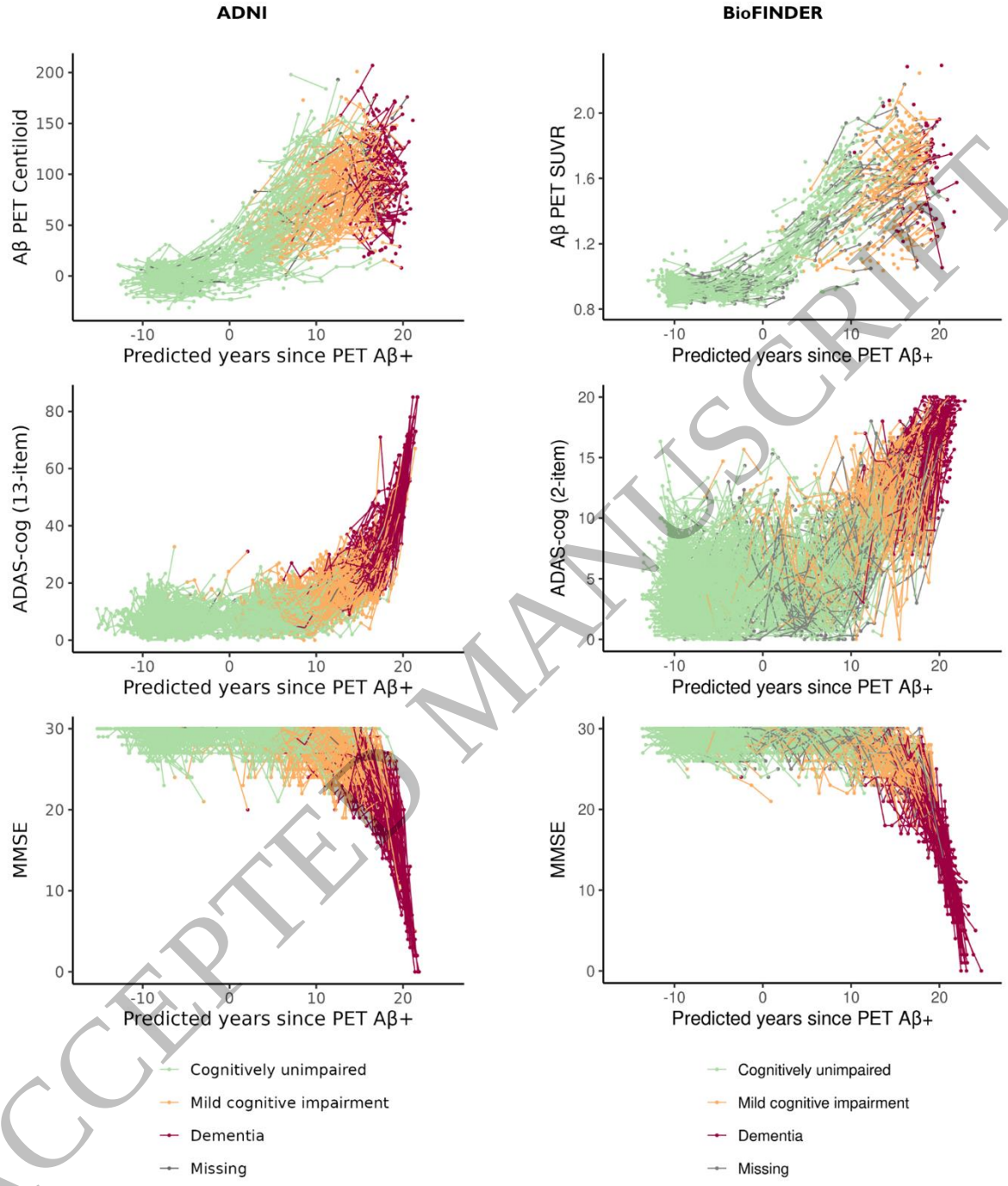

Figure 2
158x185 mm (x DPI)

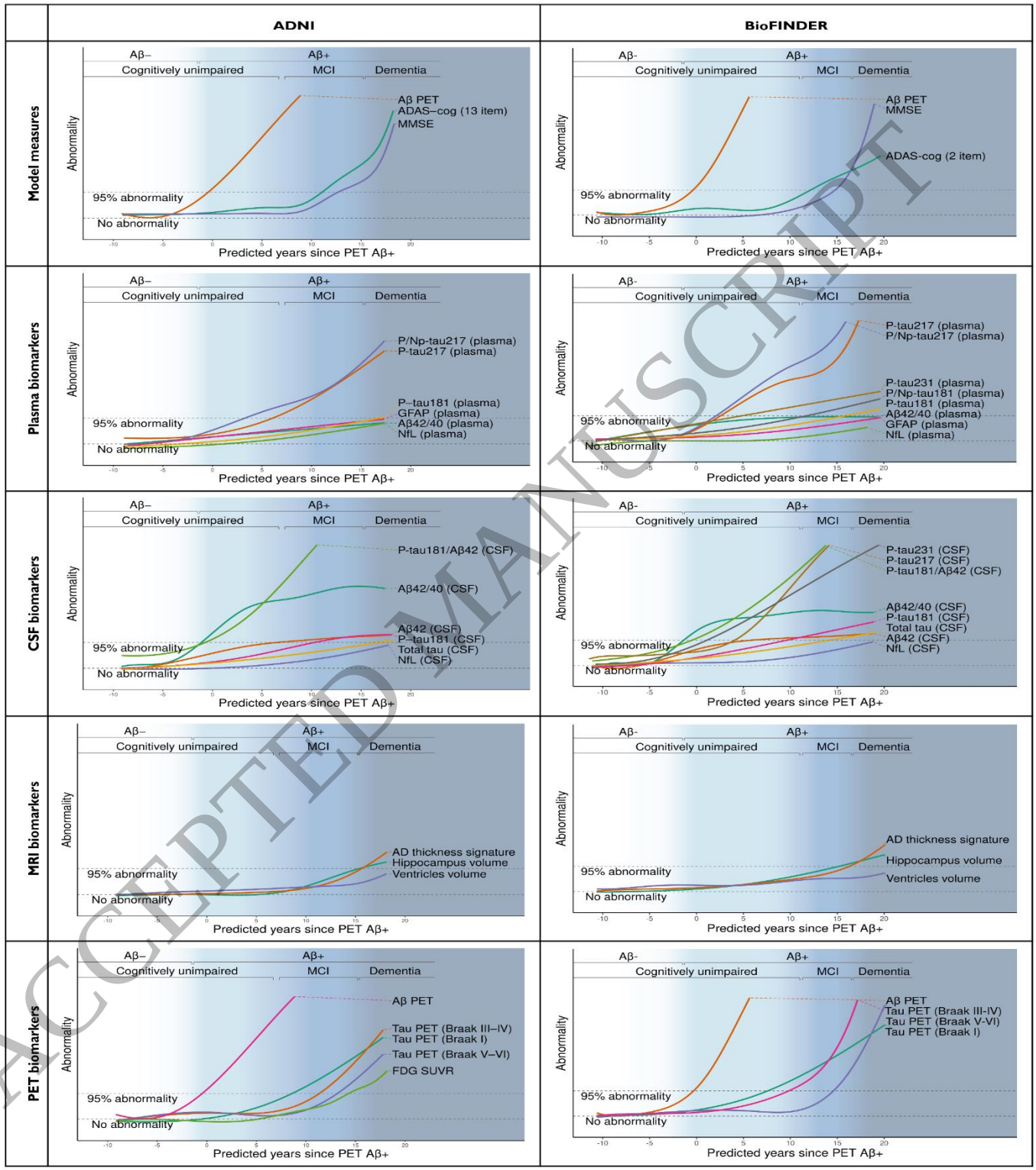

Figure 3
242x334 mm (x DPI)

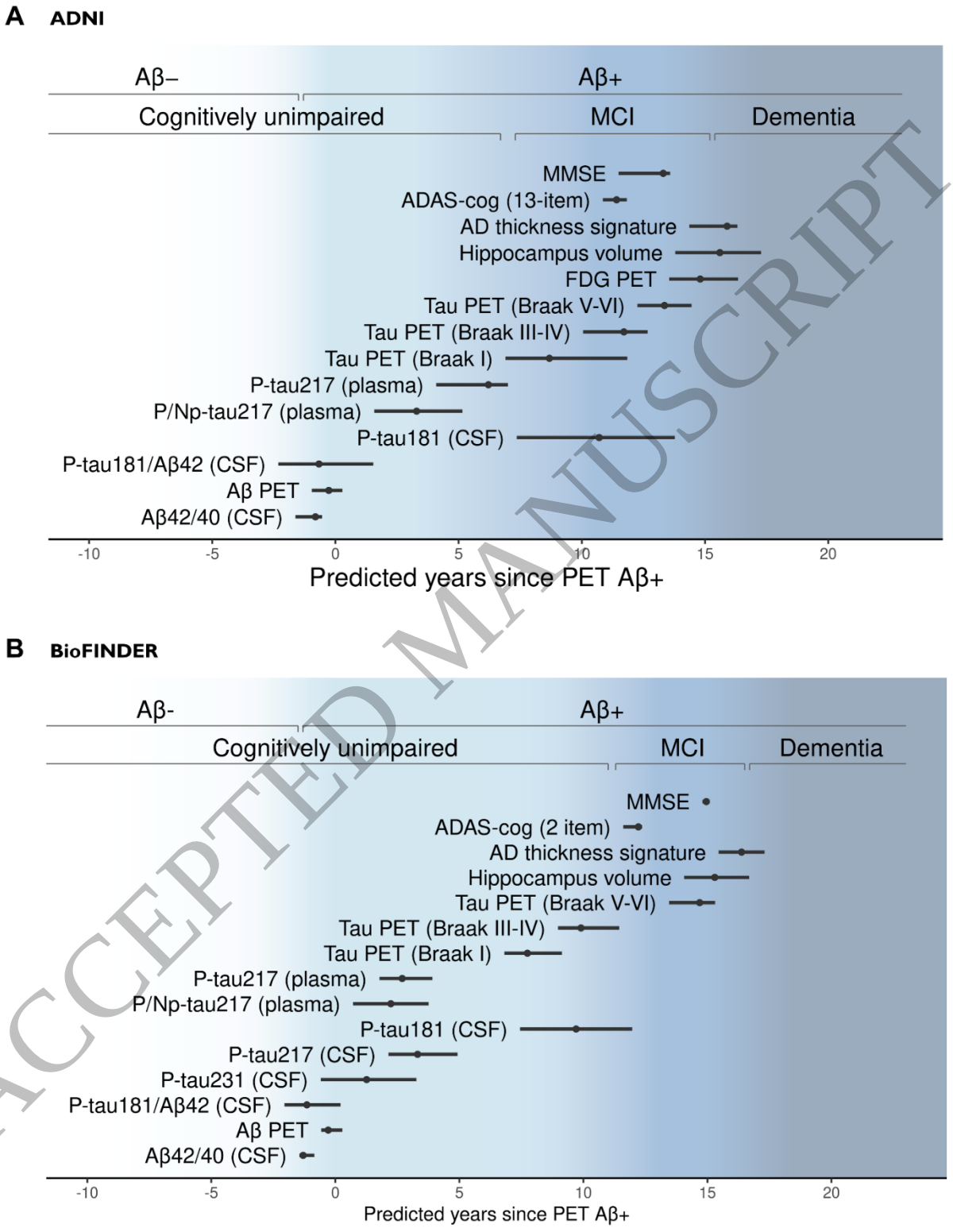

Figure 4
181x235 mm (x DPI)